Responses to RC1:

General comments:

This manuscript applies multiple linear regression (MLR) to monthly mean zonal wind data in the stratosphere, mesosphere, and lower thermosphere obtained from SABER observations, MF and meteor radar observations, and MERRA2 meteorological reanalysis to examine the effects of QBO, ENSO, and solar activity as well as seasonal changes and long-term trends. Although many similar studies based on the MLR analyses have been conducted using long-term meteorological reanalysis data, there have been few research above the stratopause due to the difficulty of observing winds. In this sense, the efforts in this manuscript are commendable. On the other hand, the method of MLR analysis and statistical significance are not well documented, and the consideration of the short data period is not sufficient. In addition, English grammar check by a native speaker is also recommended. Therefore, I think that this manuscript needs substantial revision before publication. Detailed comments are given below.

Response: Thanks for your valuable comments on our manuscript. The main improvements in this version are:

(1) To elucidate the MLR model better and to remove the collinearity of predictors, the seasonal variations and the responses of winds to F10.7, QBO_{30} (QBOA), QBO_{10} (QBOB), and MEI are retrieved through three steps. Each step has specific purpose and formulae. We note that although the procedures of applying MLR is changed from that in the last version, this does not change the main results and conclusions significantly.

(2) The statistical significance is estimated by p-value, which is used to replace the standard deviation in the last version.

(3) We applied the new MLR procedure to the 40 years of MERRA2 data (MerU40) and compared with the 18 years of MERRA2 data (MerU18). Below ~55 km, the consistencies of the responses of MerU18 and MerU40 to QBOA and ENSO are better than those to F10.7 and the linear variations. Moreover, at ~40 km and above the equator, the significant negative linear variations of MerU40 coincide well with those MerU18.

(4) The impacts of major SSWs (2003, 2005, 2006, 2007, 2009, 2010, 2013, 2018, 2019) on the trend and responses have been checked in winter months (December, January, February) and in the annual mean. Here the SSW events are adopted from Chemical Sciences Laboratory of NOAA (https://csl.noaa.gov/groups/csl8/sswcompendium/majorevents.html).

(5) English grammar is improved.

Please see the point-to-point responses below.

Major comments:

1. Time interval of the data: It seems that 18 years are too short to fit the 11-year solar cycle. Although the authors evaluated its impacts by changing the time interval, half or more of the data periods overlap, which does not seem very meaningful. Rather, a comparison using 40 years of MERRA2 data would be more meaningful. As the authors say, the MLS has been assimilated since 2004, but its effect appears to be strong only for the vertical structure of temperature, not so much for the meridional gradient of temperature and the distribution of zonal wind that is related to the meridional gradient of temperature.

Response: Following your suggestion, we have performed the new MLR procedure (see details in Respons#2 and in the text) on the 40 years (1980–2019) of MERRA2 data (MerU40). The monthly zonal mean wind at 25°S and 50 km is taken as an example to show the de-seasonalized results (Fig. R1) and MLR results (Fig. R2).
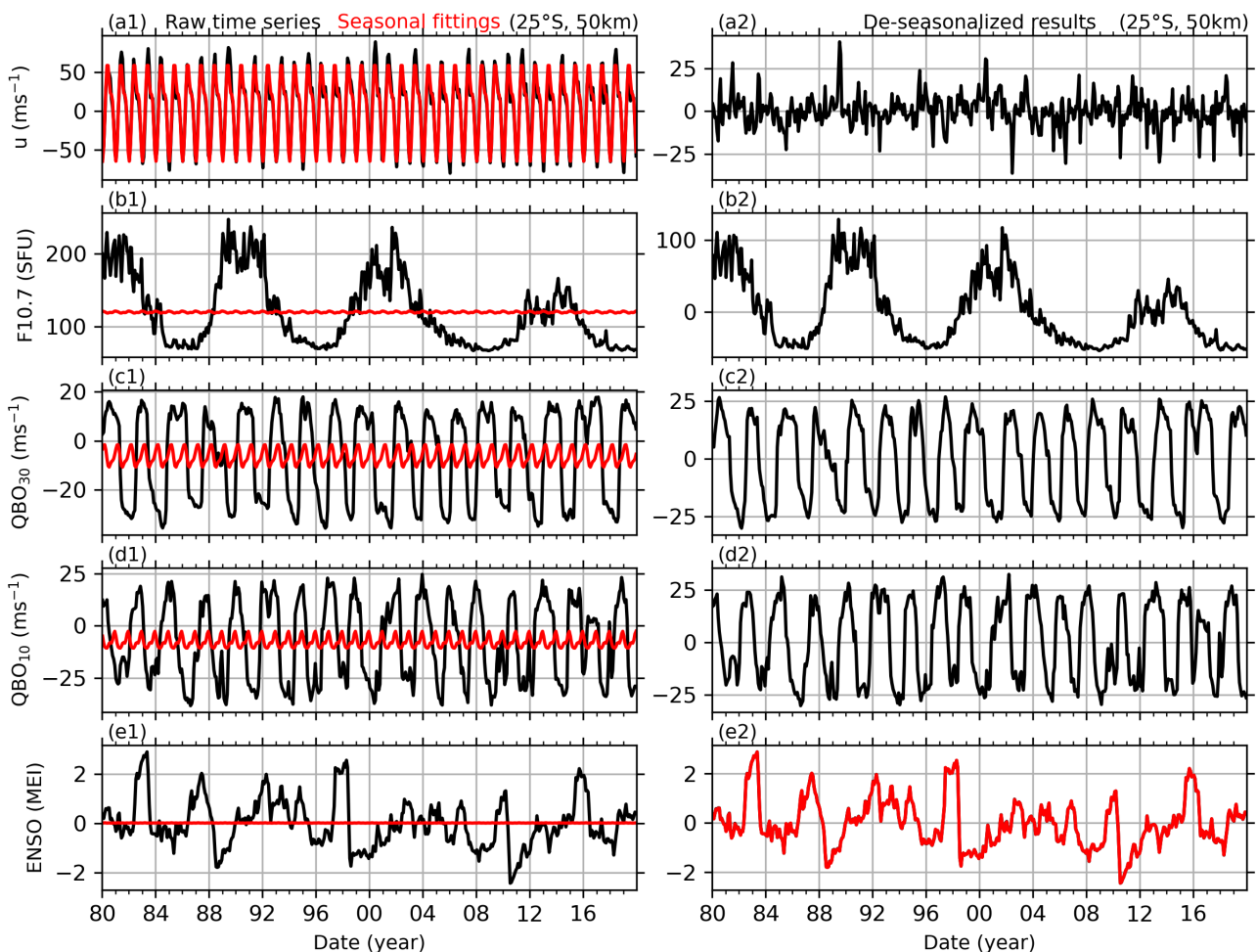
Figure R1: Example of the reference time series (left column) and their de-seasonalized results (right column). The first row: BU at 25°S and 50 km (black line in a1) and its seasonal fitting result (red line in a1), and the residual of BU (black line in a2). The second, third, and fourth rows: same captions as the first row but for solar activity (indicated by F10.7), QBO at 30 hPa (QBO$_{30}$ or QBOA) and at 10 hPa (QBO$_{10}$ or QBOB), and ENSO (indicated by MEI index). The red line in e2

is the residual of MEI index after removing the response of MEI to F10.7.

Figure R1 shows that the seasonal variations are important in the wind (Fig. R1a1 and a2) but are insignificant in the time series of F10.7, QBO$_{30}$ (QBOA) , QBO$_{10}$ (QBOB), and ENSO (Fig. R1b1-e2). Figure R2a1 shows that the responses of MerU40 to F10.7 are significant (p-value $\leq$ 0.1) in March, April, and August. This is different from the responses of the 18-year data (short for MerU18) to F10.7, which are significant only in May. The responses of MerU40 to QBOA and QBOB (Fig. R2b1) are significant in April–June and in October. This is similar to those of MerU18, which are also significant in May–June, but insignificant in April and October. The responses of MerU40 to ENSO (Fig. R2c1) are negative and significant in January–April and December. However, the responses of MerU18 to ENSO are also negative but are insignificant. The linear variations of MerU40 (Fig. R2d1) are significant in March and April (positive values) and in November and December (negative values). However, the responses of MerU18 are insignificant (judged by p-value > 0.1) in all months.
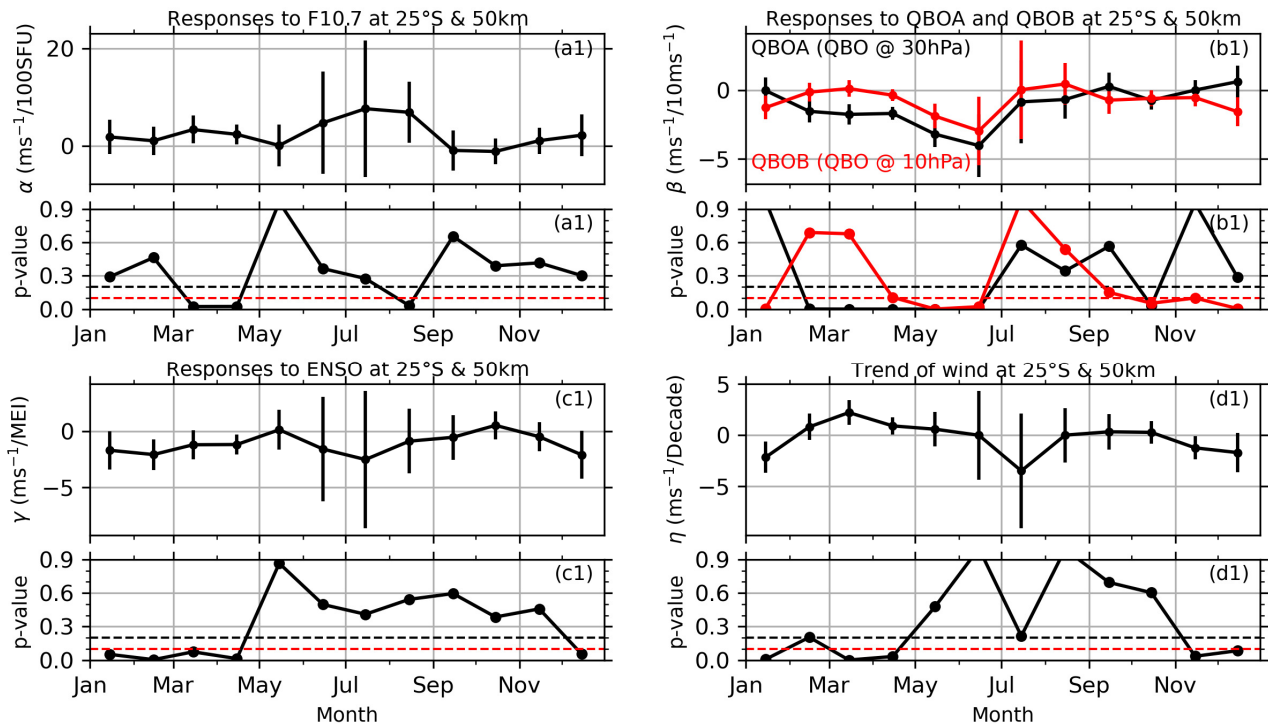
Figure R2: Example of retrieving the monthly responses of MerU40 at 25°S and 50 km (upper subplot of each panel) and their p-values (lower subplot of each panel) to solar activity (a1 and a2) QBOA (black in b1 and b2) and QBOB (red in b1 and b2), ENSO (c1 and c2), and the linear variations (d1 and d2). The error bars are the confidence interval at 90% confidence level. The red and black dashed lines indicate the p-values of 0.1 and 0.2, respectively.

Figure R3 shows the seasonal variations of MerU40 (upper row) and the responses of MerU40 (middle row) and MerU18 (lower row) to various predictors. We see that AO, SAO, and TAO of

MerU40 exhibit similar latitude-height distributions as those of the MerU18. The responses of MerU40 to QBOA are similar to those of MerU18 on the aspects of magnitudes and patterns but have a wider significant region around the equator. Around the equatorial region, the responses of MerU40 to ENSO have similar patterns to those of MerU18 around the equatorial region. However, the positive responses of MerU40 to ENSO are stronger (weaker) than those of MerU18 below ~30 km (around ~40–45 km). Around ~20°S and above ~55 km, the negative responses of MerU18 to ENSO are stronger than those of MerU40. At ~40°S and around ~30 km, the significant positive responses of MerU18 to ENSO cannot be seen in those of MerU40. The significant responses of MerU18 to F10.7 occur in wider height ranges as compared to those of MerU40 around the equator. Moreover, at latitudes higher than 30°S, the responses of MerU18 to F10.7 are negative as compared to the positive responses of MerU40 to F10.7. At around 40°N and ~40–60 km, the positive responses of MerU18 to F10.7 are weaker and less significant than those of MerU40. The linear variations of MerU18 coincide with those of MerU40 above ~30 km, except around ~45°N/S, where the negative linear variations of MerU40 (MerU18) are significant (insignificant). Below ~30 km, the positive linear variations of MerU40 extend to wider latitudes as compared to those of MerU18.
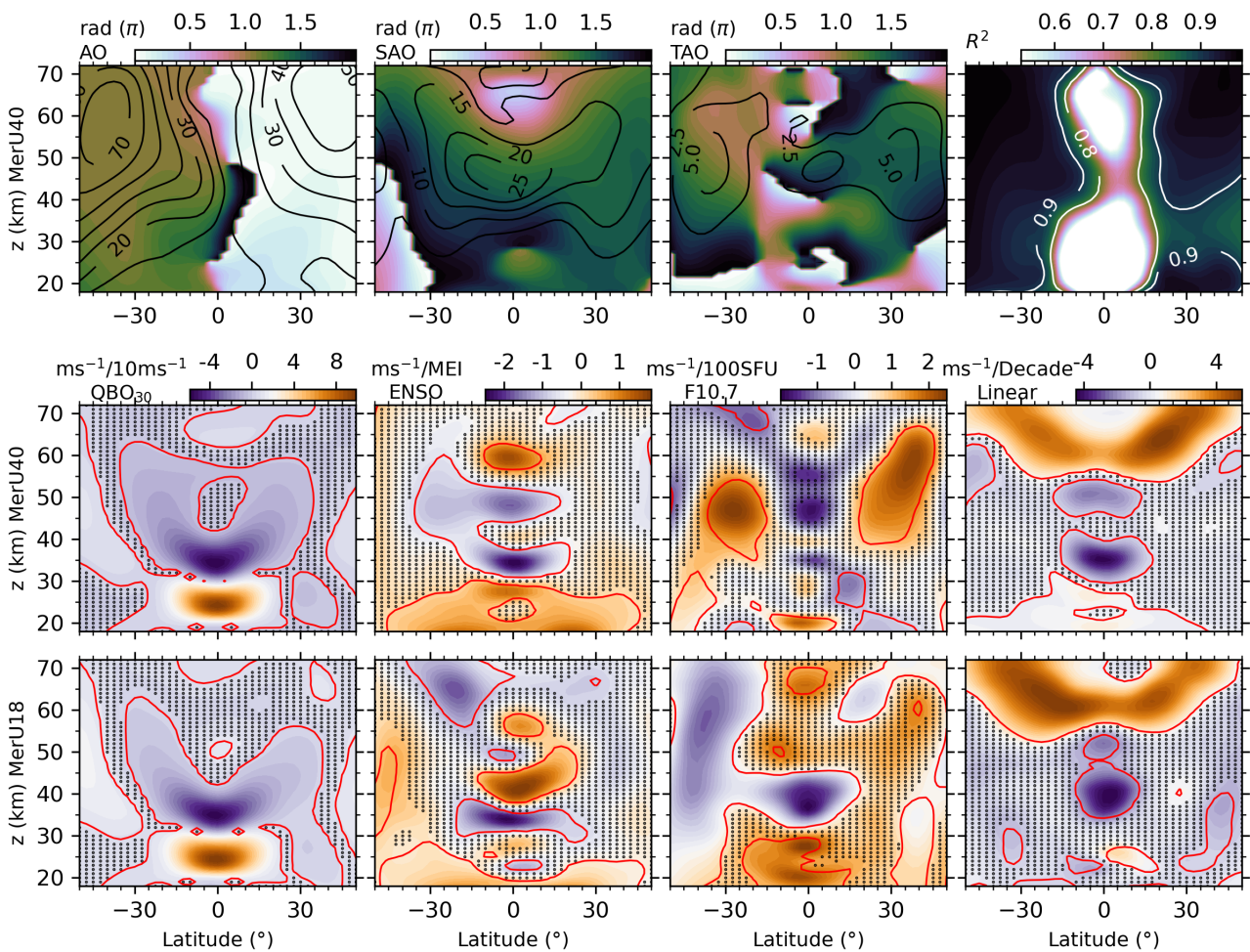
Figure R3: Upper row: the latitude-height distributions of the amplitudes (contour lines) and

phases (color scale) of seasonal variations and the R^2 scores (from left to right) of MerU40. Middle row: the latitude-height distributions of the responses of MerU40 to QBOA, ENSO, F10.7 and linear variations (from left to right). Lower row: same caption as the middle row but for the MerU18. The black dots indicate that the regression coefficients with p-values larger than 0.2. The red lines indicate the regression coefficients with p-values of 0.1.

A summary of the responses and linear variations of MerU18 and MerU40 below ~55 km (this is most reliable height since the damping is significant above this height (Ern et al., 2021)) is below. **The consistencies of the responses of MerU18 and MerU40 to QBOA and ENSO are better than those to F10.7 and the linear variations. Moreover, at ~40 km and around the equator, the significant negative linear variations of MerU40 coincide well with those MerU18.**

2. Method of MLR analysis: From the explanation in section 2.2, it appears that eq. (2) is applied to data for 216 months over 18 years, in which case only one regression coefficient is obtained for the entire period. On the other hand, section 3 shows that regression coefficients were obtained for each month, suggesting that eq. (2) without including the seasonal variation term was actually applied to 18 years of data for each month. In that case, I do not know how the seasonal variation was estimated. The authors need to properly explain the MLR method.

Response: You are right. In the last version, the regression model is,

$$u(t_i) = A_0 + \text{Season}(t_i) + \alpha\text{F10.7}(t_i) + \beta_{30}\text{QBO}_{30}(t_i)$$
$$+\beta_{10}\text{QBO}_{10}(t_i) + \gamma\text{ENSO}(t_i) + \eta t_i + \text{Res}(t_i). \tag{R1}$$

Equation R1 is applied to data for 18 years. Moreover, the regression coefficients $\alpha, \beta_{30}, \beta_{10}, \gamma, \eta$ are not specific numbers but depend on the month. They have the form of (for example, α):

$$\alpha = \alpha_0 + \sum_{k=1}^{3}[\alpha_{2k-1}\cos(k\omega t_i) + \alpha_{2k}\sin(k\omega t_i)]. \tag{R2}$$

Here, $\omega = 2\pi/12$ (month). The regression coefficient of F10.7 in January is obtained by setting $t_i = 1$ in Eq. R2. In a same way, the regression coefficient in February can be obtained by setting $t_i = 2$ in Eq. R2, and so on. Then we can get the regression coefficients in 12 months. The annual mean regression coefficient is obtained by averaging the regression coefficients in 12 months. Moreover, Eq. R1 and R2 play a role of de-seasonalizing regressor and predictors. This method was proposed by Randel and Cobb (1994) (Eq. 1 and 2 of their paper) and other researchers due to its highly compactable and portable in applications.

In this version, to easily explain the MLR model and to remove the collinearity of predictors, the seasonal variations and the responses of wind to F10.7, QBOA, QBOB, and MEI are retrieved through three steps. Each step has specific purpose and formulae. The detailed revision has been made in the text:

The detailed applications of MLR to retrieve the seasonal variations of winds and the responses of winds to F10.7, QBOA, QBOB, and MEI can be ascribed to the following three steps. For illustrative purpose, BU at 25°S and 50 km (black in Fig. R4a1) is taken as an example to show the procedure of MLR. This procedure is also applied to winds at other latitudes and heights, but results in different regressions coefficients due to the latitudinal and height dependencies of the seasonal variations and the responses of winds to F10.7, QBOA, QBOB, and MEI.
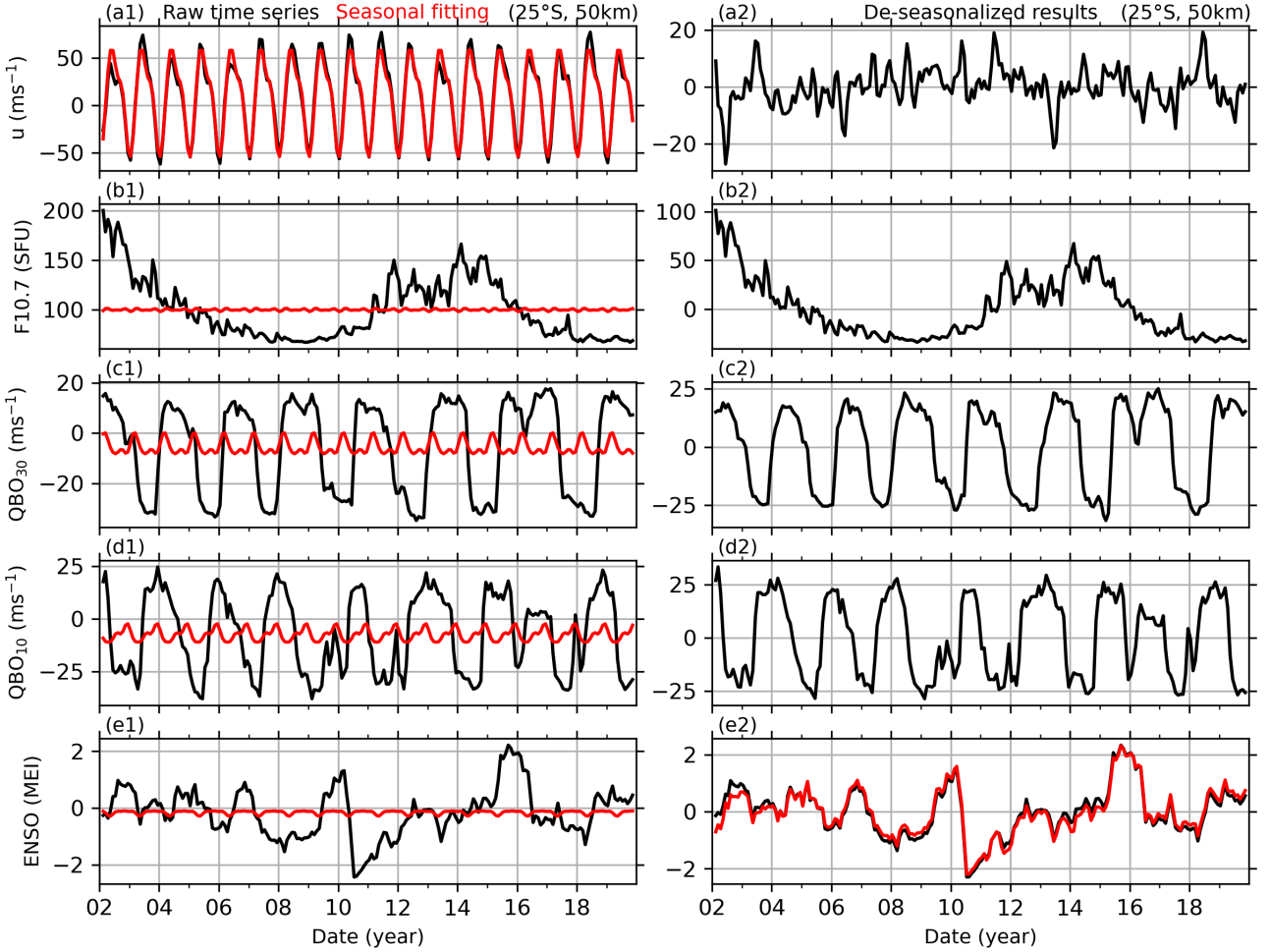
Figure R4: Same caption as Fig. R1 but for the BU at 25°S and 50 km during 2002–2019.

First, we de-seasonalize the wind and reference time series by fitting the following harmonics through the least squares method. At each latitude and height, the wind series is fitted as,

$$u(t_i) = u_0 + \sum_{k=1}^{3} A_k \cos[k\omega(t_i - \varphi_k)] + u_{res}(t_i). \qquad (R3)$$

Here, t_i ($i = 1, 2 \cdots, N$) is the month number since February 2002. u_0 is the mean wind in the entire temporal interval, u_{res} is the de-seasonalized wind. $\omega = 2\pi/12$ (month), A_k and φ_k are the amplitude and phase of the annual (AO, $k = 1$), semiannual (SAO, $k = 2$), and terannual (TAO, $k = 3$) oscillations, respectively. In the same way, Eq. R3 is used to de-seasonalize the reference time series of F10.7, QBOA, QBOB, and MEI (shown in the left column of Fig. R4), and thus their residuals (F10.7$_{res}$, QBOA$_{res}$, QBOB$_{res}$, MEI$_{res}$, shown in the right column of Fig. R4) can be

obtained and will be used as predictor variables (or explanation variables) after checking and removing their multicollinearity.

The rationality or goodness of the seasonal fitting result is quantified by R^2 score, which is the variations of the raw data explained by the model and defined as follows:

$$R^2 = 1 - \{\sum_{i=1}^{N} u_{res}^2(t_i)/\sum_{i=1}^{N}[u(t_i) - \bar{u}]^2\}, \ \bar{u} = \frac{1}{N}\sum_{i=1}^{N} u(t_i). \tag{R4}$$

The best fitting results in $R^2 = 1$, which means that the fitting result is the same as the raw data. For example, the seasonal fitting of BU at 25°S and 50 km is shown as red line in Fig. R4(a1). It coincides well with the raw BU series (black line in Fig. R4a1) with $R^2 = 0.967$. This means that Eq. R3 explains 96.7% of the variations of BU at 25°S and 50 km. Moreover, for this case, the fitting result shows that the AO has amplitude of 53.9 ms^{-1} and is in the dominant position. Then the SAO has a smaller amplitude of 13.2 ms^{-1}. While the TAO is the weakest and has amplitude of 3.9 ms^{-1}. The rationality of the fitting results (R^2) at other latitudes and heights will be shown in Sect. 3.1.

Table 1: The correlation coefficients and their p-values of regressors

	QBO$_{30}$		QBO$_{10}$		ENSO (MEI indx)	
	CC	p-value	CC	p-value	CC	p-value
F10.7	-0.0283	0.6803	0.0003	0.9965	0.2022	0.0030
QBO$_{30}$			-0.0025	0.9705	0.0368	0.5921
QBO$_{10}$					-0.0779	0.2567

Second, we check the multicollinearity among the predictor variables, which are the de-seasonalized F10.7, QBO$_{30}$, QBO$_{10}$, and MEI. The multicollinearity often leads to meaningless results if the correlation coefficients (CCs) between two or more predictor variables are significant. Here we calculate the CC and p-value of each pair of predictor variables (Table 1). If the p-value of a pair of predictor variables is less than 0.1 (or 0.05), one can state that the CC differs from zero at a confidence level 90% (or 95%). And thus, the multicollinearity of this pair is significant. In contrast, larger p-values indicate lower confidence level and insignificant multicollinearity. Table 1 shows that, the CCs of most pairs are less than 0.1, and p-values are larger than 0.1. This indicates that the multicollinearities of these pairs are insignificant and are approximately independent. On exception is the pair of F10.7 and ENSO, which has a CC of 0.2022 with p-value of 0.0030. This indicates that the multicollinearity of F10.7 and ENSO is significant at confidence level of 95%. To improve the independency between F10.7 and ENSO, a linear regression is performed with response variable of MEI index and predictor variable of F10.7. The residual of MEI index, which excludes the influences of F10.7, is used as a predictor variable to represent the effects of ENSO in the following

MLR model. We note that the residual of MEI index is still noted as MEI_{res} in the following text. Now, the multicollinearity among the four predictor variables can be neglected and ensures a meaningful result of MLR in the next step.

Third, MLR is applied to get the responses of the de-seasonalized winds (i.e., u_{res} in Eq. R3) to the four predictor variables (F10.7_{res}, QBOA_{res}, QBOB_{res}, MEI_{res}) prepared in the second step. The MLR model is written as:

$$u_{res}(t_i) = \alpha \text{F10.7}_{res}(t_i) + \beta_A \text{QBOA}_{res}(t_i) + \beta_B \text{QBOB}_{res}(t_i) + \gamma \text{MEI}_{res}(t_i) + \eta t_i + \varepsilon(t_i) \quad (R5)$$

The regression coefficients $\alpha, \beta_A, \beta_B, \gamma$ indicate the responses of wind to F10.7, QBOA, QBOB, and MEI, respectively. The regression coefficient η is the linear variations or long-term trend. $\varepsilon(t_i)$ is the residual of the fitting and can be used to estimate the standard deviation and the p-value of each coefficient with the help of variance-covariance matrix and student-t test (Kutner et al., 2004; Mitchell et al., 2015). The monthly responses are obtained by selecting t_i in Eq. (R5) only in that month of each of year. E.g., the response in January can be obtained by selecting the data only in January of each year. The annual responses are obtained by using all the data during 2002–2019.

3. Multicollinearity: In the MLR analysis, multicollinearity often leads to meaningless results. The authors need to evaluate and indicate whether the correlations between regressors are sufficiently small before performing the MLR analysis.

Response: Following your suggestion, we have evaluated the multicollinearity of each pair of regressors in this version. Please see the second step in Responses#2 and in Sec. 2.2 of the text. We rewrite here to close the responses:

Table 1: The correlation coefficients and their p-values of regressors

	QBO$_{30}$		QBO$_{10}$		ENSO (MEI indx)	
	CC	p-value	CC	p-value	CC	p-value
F10.7	-0.0283	0.6803	0.0003	0.9965	0.2022	0.0030
QBO$_{30}$			-0.0025	0.9705	0.0368	0.5921
QBO$_{10}$					-0.0779	0.2567

Here we calculate the CC and p-value of each pair of predictor variables (Table 1). If the p-value of a pair of predictor variables is less than 0.1 (or 0.05), one can state that the CC differs from zero at a confidence level 90% (or 95%). And thus, the multicollinearity of this pair is significant. In contrast, larger p-values indicate lower confidence level and insignificant multicollinearity. Table 1 shows that the CCs of most pairs are less than 0.1, and p-values are larger than 0.1. This indicates that the multicollinearities of these predictor variables are insignificant and are approximately independent. On exception is the pair of F10.7 and ENSO, which has a CC of 0.2022 with p-value of 0.0030. This indicates that the multicollinearity of F10.7 and ENSO is significant at confidence

level of 95%. To improve the independency between F10.7 and ENSO, a linear regression is performed with response variable of MEI index and predictor variable of F10.7. The residual of MEI index, which excludes the influences of F10.7, is used as a predictor variable to represent the effects of ENSO in the following MLR model.

4. Statistical significance: In this manuscript, the regression coefficient is considered statistically significant if it is greater than 1σ. However, there is no description of how σ is calculated. In addition, when determining whether a regression coefficient is statistically significant in the MLR analysis, it is common practice to use the p-value of each regression coefficient. Unless there is a special reason to use σ, the p-value should be used (e.g., Mitchell et al. (2015)).

Response: Following your suggestion, we have used the p-value to determine whether a regression coefficient is statistically significant in the new version.

The standard deviation is calculated by the variance-covariance matrix and the residuals of the MLR model (Chapter 6 of Kutner et al. (2004). For a MLR model of,

$$Y_{n\times 1} = X_{n\times p}B_{p\times 1} + \epsilon$$

Here $X_{n\times p}$ is the predictor matrix with p columns (the number of predictor variables) and n rows (observation times or sampling points). $Y_{n\times 1}$ is the response variable with observations times of n. $B_{p\times 1} = \{b_i: i = 0, 1, \cdots, p-1\}$ is the expected regression coefficients of predictor variables. ϵ is a vector of independent normal random variables. Due to the estimated $B_{p\times 1}$ by MLR model is unbiased, the variance-covariance matrix of $B_{p\times 1}$,

$$s^2\{B\}_{p\times p} = \begin{bmatrix} s^2\{b_0\} & s\{b_0, b_1\} & \cdots & s\{b_0, b_{p-1}\} \\ s\{b_1, b_0\} & s^2\{b_1\} & \cdots & s\{b_1, b_{p-1}\} \\ \vdots & \vdots & & \vdots \\ s\{b_{p-1}, b_0\} & s\{b_{p-1}, b_1\} & \cdots & s^2\{b_{p-1}\} \end{bmatrix} = \frac{\sum_{j=1}^{n} \epsilon_j^2}{n-p} \cdot (X'X)^{-1}$$

The significance of the difference between b_i and 0 can be estimated by student-t test. For the confidence level of $1-\alpha$, student-t test states that,

$$\begin{cases} |b_j/s\{b_j\}| \leq t(1-\alpha/2; n-p), & b_i = 0 \\ |b_j/s\{b_j\}| > t(1-\alpha/2; n-p), & b_i \neq 0 \end{cases}.$$

Then the p-value is calculated from t-distribution table with $n-p$ degrees of freedom and α, that describes how likely to find a particular set of observations if the null hypothesis (i.e., the regression coefficient is 0) were true. The smaller the p-value, the more likely to reject the null hypothesis and accept the no-null hypothesis (i.e., the regression coefficient is significant)

5. Impact of SSW: In general, if the effect of SSW is large, it should occur that the regression coefficient is not statistically significant despite its large value. The authors should first check to see

if this is the case, especially in the high latitudes of the winter northern hemisphere.

Furthermore, it is questionable whether it makes sense to apply the MLR analysis to spline interpolated data. Also, it should be explicitly stated which latitude bands were replaced by spline interpolation. Looking at Fig. 10c, it appears that all winters were replaced by spline interpolation, but major SSW does not occur every year. It should be explicitly stated by what criteria SSW is defined.

Response: Following your suggestion and according the $|BU_{Res}|$ shown in Fig. 10 of the new version, we reconstruct the BU at 30°N–50°N and throughout the height range.
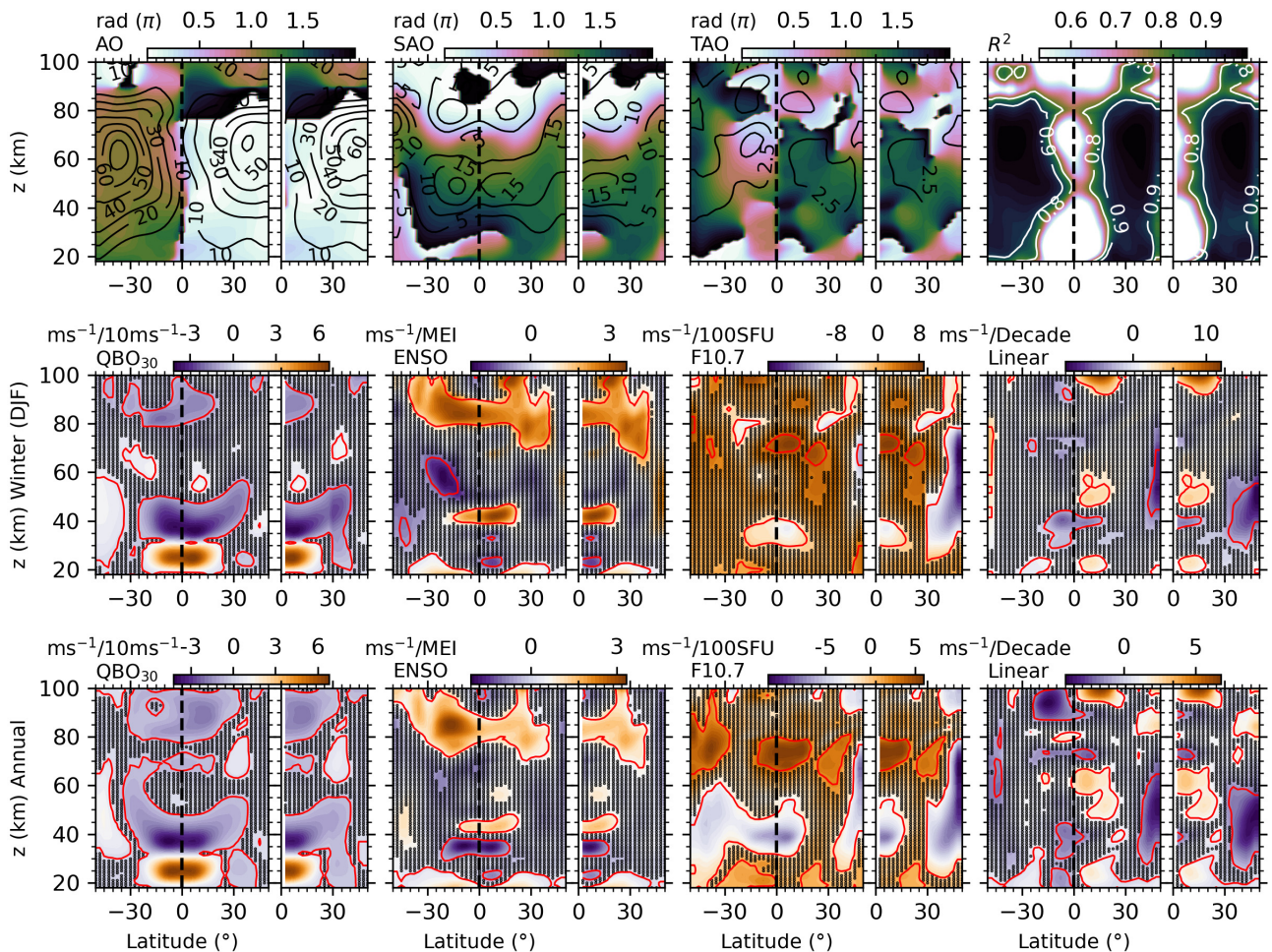
Figure R5: Regression results of the raw (50°S–50°N, left panel of each subplot) and reconstructed BU (0°–50°N, right panel of each subplot) in the NH during 2002–2019. Upper row: seasonal variations. Middle row: the responses of BU to QBO30, QBO10, ENSO, F10.7 and linear variations (from left to right) in winter (December-January-February). Lower row: same caption as the middle row but for those of the annual mean.

According to the major SSW events released by the Chemical Sciences Laboratory of NOAA, (https://csl.noaa.gov/groups/csl8/sswcompendium/majorevents.html), We reconstructed BU only in the winters when the major SSWs occurred (2003, 2004, 2006, 2007, 2008, 2009, 2013, 2018,

2019). Figure R5 shows the amplitudes of seasonal variations and R^2 scores (the first rows), and the responses of reconstructed winds to QBO, ENSO, F10.7, and the linear variations of the raw and reconstructed BU in winter (the second row) and in the annual mean (the third row).

The annual mean responses of the reconstructed and raw BU to QBO_{30} and ENSO are similar on the aspects of both patterns and magnitudes. In contrast, at ~30–60 km and latitudes higher than 30°N, the annual mean responses of the reconstructed BU to F10.7 are more negative and cover a wider region as compared to those of the raw BU. The linear variations of the reconstructed winds are more negative at latitudes higher than 30°N at compared to those of the raw BU.

This has been added in the text.

Minor comments:

6. L. 143-145: Is it safe to consider data from a single point observation as the same as the zonal average, even though it is a monthly average? For example, how does this compare to the data of Smith et al. (2017)?

Response: This point should be clarified. Figure R6 shows the balance winds at the equator reported by Liu et al. (2021) and Smith et al. (2017). It can be seen that the two datasets show a good consistency below ~80 km.

The monthly average of single point observation eliminates the aliasing from migrating tides and traveling planetary waves but contains the non-migrating tides and stationary planetary waves. For the consistency of balance wind and the monthly averaged zonal wind observed at a single station, Figure 3 of Smith et al. (2017) showed that the monthly zonal wind from a meteor radar at Ascension Island (8ºS) coincides well with the balance wind at 81 and 84 km. This indicates that the monthly averaged zonal wind at a single station can represent the zonal average at least below 84 km. While above 84 km, the left column of Figure R6 shows that the theoretical balance winds are mainly eastward (upper panel (a) of the left column). In contrast, the reconstructed winds from a meteor radar observation at Koto Tabang (0.2ºS) are mainly westward. The differences between the theoretical balance wind and meteor radar observations are mainly the tidal aliasing above 84 km (Hitchman and Leovy, 1986; Smith et al., 2017; Xu et al., 2009). Moreover, the comparisons between the reconstructed balance winds with UARP (Atmosphere Research Satellite Reference Atmosphere Project wind climatology) and HWM14 (Horizontal Wind Model, Version 2014) exhibited general consistency above 80 km (Figures 6 and 7 of Liu et al., 2021).

Since the contaminations by non-migrating tides and stationary planetary waves cannot be removed through monthly average at a single station in theory, further validation should be performed by comparing the monthly averaged winds at different longitudes but similar latitudes.
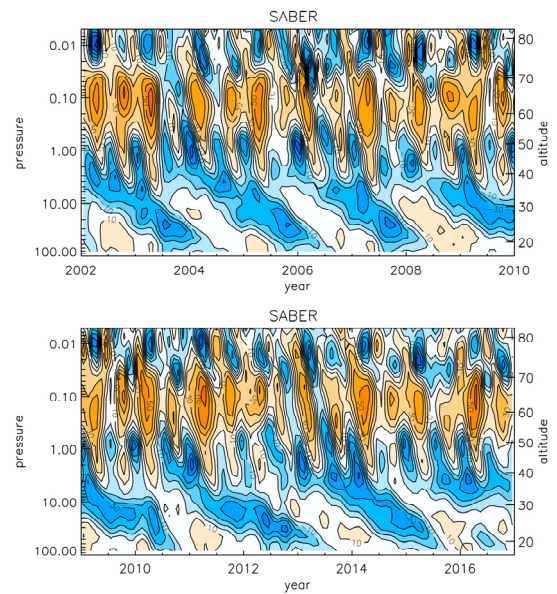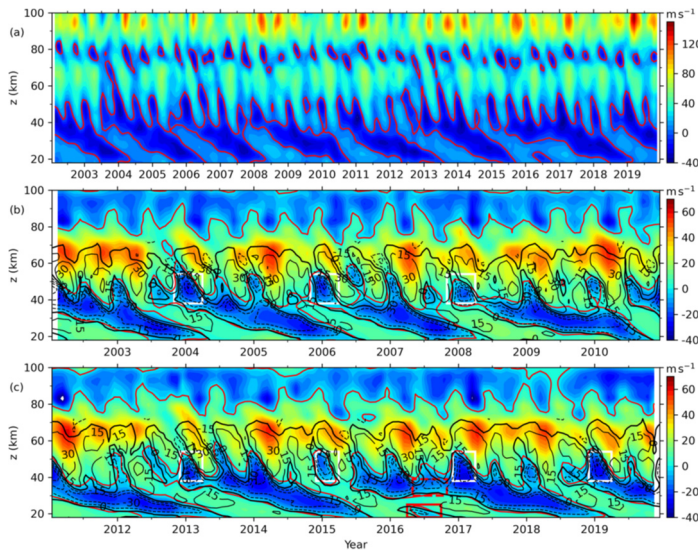
Figure R6: Balance winds at the equator reported by Liu et al. (2021, left column) and Smith et al. (2017, right column). The panel (a) of left column shows the theoretical balance winds from 18 to 100 km. The panels (b) and (c) the reconstructed balance wind, which is the wind in panel (a) replaced by the meteor radar observations at Koto Tabang (0.2ºS) above 80 km.

In the text, we have revised this point as "For the consistency of BU and the monthly averaged zonal wind observed at a single station, Figure 3 of Smith et al. (2017) showed that the monthly zonal wind from a meteor radar at Ascension Island (8ºS) coincides well with the BU at 81 and 84 km. This indicates that the monthly averaged zonal wind at a single station can represent the zonal average at least below 84 km. While above 84 km, Fig. 2(a) of Liu et al. (2021) shows that the theoretical balance winds are mainly eastward. In contrast, the reconstructed winds (Fig. 2b and 2c of Liu et al. (2021)) from a meteor radar observation at Koto Tabang (0.2ºS) are mainly westward. The differences between the theoretical balance wind and meteor radar observations are mainly the tidal aliasing above 84 km (Hitchman and Leovy, 1986; Smith et al., 2017; Xu et al., 2009)"

7.   Fig. 2: It is hard to see the phases from the arrows. I recommend to show the amplitudes by contours and the phases by colors.

   Response: Following your suggestion, we have revised Fig.2 (Fig. 3 of this version), which shows the amplitudes by contour lines and phases by colors. Please see Fig. R7 below.
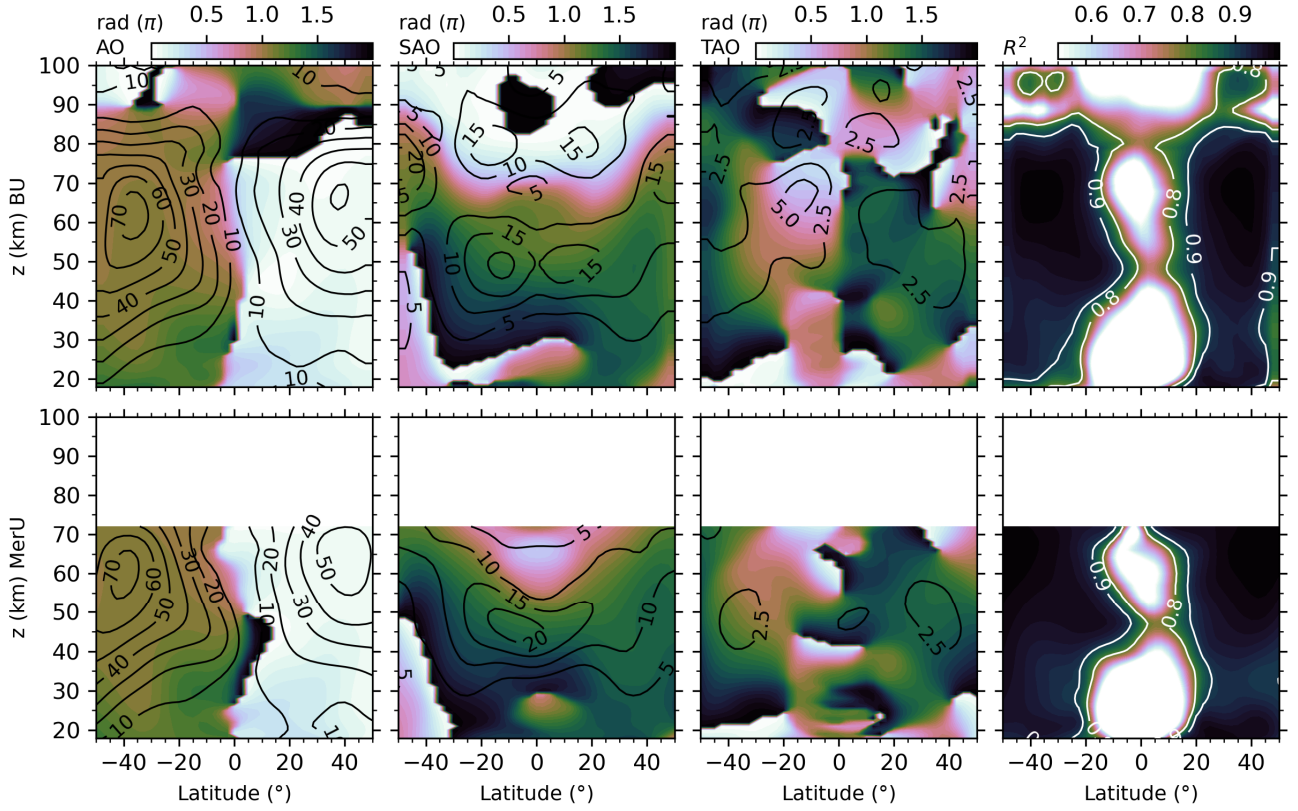
Figure R7: The latitude-height distributions of the amplitudes (contour lines) and phases (color scale) of seasonal variations and the R^2 scores (from left to right) of BU (upper row) and MerU (lower row).

8. L. 237: Please clarify how the annual mean response was calculated. Is it an annual mean of the regression coefficient for each month? Or did you apply the MLR to the data including whole months (216 months)?

    Response: In the last version, the regression model is,

$$u(t_i) = A_0 + \text{Season}(t_i) + \alpha\text{F10.7}(t_i) + \beta_{30}\text{QBO}_{30}(t_i)$$
$$+\beta_{10}\text{QBO}_{10}(t_i) + \gamma\text{ENSO}(t_i) + \eta t_i + \text{Res}(t_i). \tag{R1}$$

Equation (R1) is applied to data for 18 years. Moreover, the regression coefficients $\alpha, \beta_{30}, \beta_{10}, \gamma, \eta$ are not specific numbers but depend on the month. They have the form of (for example, α):

$$\alpha = \alpha_0 + \sum_{k=1}^{3}[\alpha_{2k-1}\cos(k\omega t_i) + \alpha_{2k}\sin(k\omega t_i)]. \tag{R2}$$

Here, $\omega = 2\pi/12$ (month). The regression coefficient of F10.7 in January is obtained by setting $t_i = 1$ in Eq. (R2). In a same way, the regression coefficient in February can be obtained by setting $t_i = 2$ in Eq. (R2), and so on. Then we can get the regression coefficients in 12 months. **The annual mean regression coefficient is obtained by averaging the regression coefficients in 12 months.**

    In this version, to better explain the MLR model and to remove the collinearity of predictors, the seasonal variations and the responses of wind to F10.7, QBO₃₀ (QBOA), QBO₁₀ (QBOB), and

MEI are retrieved through steps. Please find details in Responses#2 and in Sec.2.2 of the text. A summary is below:

First, we de-seasonalize the wind and reference time series by fitting the seasonal variations through the least squares method.

Second, we check the multicollinearity among the predictor variables, which are the de-seasonalized F10.7, QBO$_{30}$, QBO$_{10}$, and MEI. The multicollinearity of F10.7 and MEI is removed through linear regression with predictor variable of F10.7 and response variable of MEI.

Third, MLR is applied to the de-seasonalized winds (i.e., u_{res} in Eq. R3) to the four predictor variables (F10.7$_{res}$, QBOA$_{res}$, QBOB$_{res}$, MEI$_{res}$) and is written as:

$$u_{res}(t_i) = \alpha \text{F10.7}_{res}(t_i) + \beta_A \text{QBOA}_{res}(t_i) + \beta_B \text{QBOB}_{res}(t_i) + \gamma \text{MEI}_{res}(t_i) + \eta t_i + \varepsilon(t_i) \quad \text{(R4)}$$

The monthly responses are obtained by selecting t_i in Eq. (R4) only in that month of each of year. E.g., the response in January can be obtained by selecting the data only in January of each year. The annual responses are obtained by using all the data during 2002–2019.

9. L. 275: higher southern (northern) latitudes in summer (winter) → higher latitudes in the winter hemisphere

Response: Following your suggestion, we have revised as "the responses extending to higher latitudes in winter hemisphere".

10. L. 275-277: I cannot see the signal at 50S/N at z=50-80 km.

Response: Indeed, the signal is weak in this region. The positive responses can be judged through p-values since the regression coefficients around zero have larger p-values, which have been indicated by black dots. In this version, the p-value of 0.1 is indicated by red contour lines. The responses at 50°S circled by the red contour lines, which extend from 30°N to 50°S. Thus, we judge that the responses at 50°S are positive. However, the responses are negative at 50°N.

We have revised in the text as "Moreover, the annual mean responses of BU and MerU to QBO$_{30}$ and QBO$_{10}$ are positive and significant at 50°S at ~z=50–80 km. In contrast, the responses of winds to QBO$_{30}$ and QBO$_{10}$ are negative and have smaller values with p-values less than 0.1".

11. L. 381-420: Trend fitting is sensitive to the values at both edge points. The authors need to mention this point.

Response: You are right. We have added this in the text as "The linear variations of both BU and MerU depend strongly on the temporal intervals and on the values at both edge points".

12. L. 455-456: I think that the seasonal asymmetry is explained by semiannual and terannual

components to some extent.

Response: Thanks for your suggestion. We have added this in the text as "The seasonal asymmetry of zonal winds might be induced by SAO and TAO".

References:

Liu, X., Xu, J., Yue, J., Yu, Y., Batista, P. P., Andrioli, V. F., Liu, Z., Yuan, T., Wang, C., Zou, Z., Li, G., and Russell III, J. M.: Global balanced wind derived from SABER temperature and pressure observations and its validations, Earth System Science Data, 13, 5643–5661, https://doi.org/10.5194/essd-13-5643-2021, 2021.

Mitchell, D.M., Gray, L.J., Fujiwara, M., Hibino, T., Anstey, J.A., Ebisuzaki, W., Harada, Y., Long, C., Misios, S., Stott, P.A. and Tan, D. (2015), Signatures of naturally induced variability in the atmosphere using multiple reanalysis datasets. Q. J. R. Meteorol. Soc., 141: 2011-2031. https://doi.org/10.1002/qj.2492

Smith, A. K., Garcia, R. R., Moss, A. C., and Mitchell, N. J.: The semiannual oscillation of the tropical zonal wind in the middle atmosphere derived from satellite geopotential height retrievals, Journal of the Atmospheric Sciences, 74, 2413–2425, https://doi.org/10.1175/JAS-D-17-0067.1, 2017.

Hitchman, M. H. and Leovy, C. B.: Evolution of the zonal mean state in the equatorial middle atmosphere during October 1978-May 1979, J. Atmos. Sci., 43, 3159–3176, https://doi.org/10.1175/1520-0469(1986)043<3159:EOTZMS>2.0.CO;2, 1986.